Chin. J. Astron. Astrophys. Vol. 5 (2005), No. 4, 327–346
(*http://www.chjaa.org*)

Chinese Journal of
Astronomy and
Astrophysics

An Analytic Model of Galactic Winds and Mass Outflows*

Cheng-Gang Shu[1,2,3], Hou-Jun Mo[3,4] and Shu-De Mao[5]

[1] Joint Center for Astrophysics, Shanghai Normal University, Shanghai 200234; *cgshu@center.shao.ac.cn*
[2] Shanghai Astronomical Observatory, Chinese Academy of Sciences, Shanghai 200030
[3] Max-Planck-Institut für Astrophysik, Karl-Schwarzschild-Strasse 1, Postfach 1317 D-85741 Garching, Germany
[4] Astronomy Department, University of Massachusetts, Amherst, MA 01003, USA
[5] Jodrell Bank Observatory, Univ. of Manchester, Macclesfield, Cheshire SK11 9DL, UK

Received 2004 December 16; accepted 2005 June 16

Abstract Galactic winds and mass outflows are observed both in nearby starburst galaxies and in high-redshift star-forming galaxies. We develop a simple analytic model to understand the observed superwind phenomenon with a discussion of the model uncertainties. Our model is built upon the model of McKee & Ostriker for the interstellar medium. It allows one to predict how properties of a superwind, such as wind velocity and mass outflow rate, are related to properties of its star-forming host galaxy, such as size, gas density and star formation rate. The model predicts a threshold of star formation rate density for the generation of observable galactic winds. Galaxies with more concentrated star formation activities produce superwinds with higher velocities. The predicted mass outflow rates are comparable to (or slightly larger than) the corresponding star formation rates. We apply our model to both local starburst galaxies and high-redshift Lyman break galaxies, and find its predictions to be in good agreement with current observations. Our model is simple and so can be easily incorporated into numerical simulations and semi-analytical models of galaxy formation.

Key words: galaxies: starburst – galaxies: ISM – galaxies: kinematics and dynamics – galaxies: formation and evolution

1 INTRODUCTION

Galactic-scale bulk motions of gas, such as galactic winds and mass outflows, have been observed both in local starbursts (Forbes et al. 2000; Heckman et al. 2000 and references therein) and in high redshift star-forming galaxies (Pettini et al. 2000, 2001; Dawson et al. 2002; Adelberger et

* Supported by the National Natural Science Foundation of China.

al. 2002). Evidence for such superwinds and mass outflows can be obtained from X-ray emission produced by the hot gas and from optical line emission from the warm gas associated with star-forming galaxies (Martin, Kobulnicky & Heckman 2002; Strickland et al. 2002). Based on medium-resolution spectra of Na D ($\lambda\lambda 5890, 5896$) and X-ray observations of some local starburst galaxies, Heckman et al. (2000) obtained wind velocities in the range $\sim 400 - 800\,\mathrm{km\,s^{-1}}$ and mass outflow rates that are comparable to star formation rates (hereafter SFRs). Using observations of nebular absorption lines and Ly-α emission lines, Pettini et al. (2000) and Adelberger et al. (2002) showed that galactic winds are common in high-redshift Lyman break galaxies. The inferred wind velocities for these objects range from several hundred $\mathrm{km\,s^{-1}}$ to about $1000\,\mathrm{km\,s^{-1}}$, with a median value of about $500\,\mathrm{km\,s^{-1}}$. For the bright gravitationally lensed Lyman-break galaxy, MS 1512-cB52 ($z = 2.72$), Pettini et al. (2000, 2001) estimated the mass outflow rate to be $\sim 60\,\mathrm{M_\odot\,yr^{-1}}$, comparable to the star formation rate of this system derived from its UV luminosity.

These bulk motions of gas (superwinds) in star-forming galaxies are believed to be driven by the kinetic energy from supernova (hereafter SN) explosions, and may change the thermal and chemical properties of the intergalactic medium (IGM) that forms galaxies (Ferrara, Pettini & Shchekinov 2000; Furlanetto & Loeb 2002). It is therefore essential to have a proper understanding of these phenomena in order to understand galaxy formation itself.

So far, our understanding of galactic superwinds is still quite incomplete since the pioneer work done by Chevalier & Clegg (1985). Recently, based on the SN remnant evolution model of McKee & Ostriker (1977), Efstathiou (2000) established a multi-phase interstellar medium (ISM) model in which galactic winds result from the expansion of hot phase gas. Combined with other physical prescriptions such as the infall of the cooling gas and star formation, he investigated the formation and evolution of disk galaxies in this model, and studied the dependence of mass outflow from a galaxy on the circular velocity of its host halo. Silk (2001, 2002) proposed an analytic model for the feedback process and the outflow in galaxies based on disk gravitational instability and multi-phase ISM. There have also been attempts to use numerical simulations to understand how galactic winds can be produced (e.g. Tomisaka & Bregman 1993; Suchkov et al. 1994; Mac Low & Ferrara 1999). However, current simulations still lack the resolution to deal with such processes as the evolution of supernova remnants and the formation of multi-phase gas that may be essential for the formation of superwinds. Because of this, simple assumptions are usually made about the superwinds when studying their impact on the IGM (e.g. Strickland & Stevens 2000; Scannapieco, Ferrara & Broadhurst 2000; Scannapieco, Ferrara & Madau 2002; Theuns, Mo & Schaye 2001; Theuns et al. 2002; White, Hernquist & Springel 2002; Bertone, Stoehr & White 2004).

In this paper, we attempt to construct a simple analytic model for galactic winds. Our model is based on the model of McKee & Ostriker (1977) for supernova evolution in the ISM. Our goal is to understand how properties of galactic winds, such as wind velocity and mass outflow rate, are related to the properties of star-forming galaxies, such as size, gas density and SFR. Although the assumptions are clearly restrictive for what is a very complicate multiphase situation in reality, the establishment of such relations will allow one to include superwinds in simulations and semi-analytical models of galaxy formation. We test our model by comparing its predictions with observations of superwinds in local starburst galaxies and in high-redshift Lyman-break galaxies. Uncertainties in the model predictions due to the simplifying assumptions are discussed.

Our basic model for the generation of superwinds is similar to that of Efstathiou (2000), as both his paper and ours are based on McKee & Ostriker (1977). While Efstathiou focused on the details regarding the assembly and star formation in two example galaxies (one dwarf-type and the other Milky-Way type), we focus on the statistical properties of superwinds in star forming

galaxies based on simple empirical models about star formation. Moreover, the implementation of the important parameter porosity Q and the prescription of the star formation are different in the present paper. In addition, we compare our theoretical predictions with observations for local starburst galaxies and high-redshift Lyman-break galaxies.

2 MODEL

In this section, we will use the model of McKee & Ostriker (1977, hereafter MO77) for supernova evolution in the interstellar medium (ISM) to construct a model of galactic winds and mass outflows for star forming galaxies. Although their model is simple, it is still a basic and successful theory for cloud evaporation due to SNe. Before going into the details, we summarize here the basic idea underlying our modelling (see also Efstathiou 2000, hereafter E2000, for more details).

In MO77, cold star-forming gas in the ISM is assumed to be in the form of cold clouds surrounded by a warm ISM with temperature of about $\lesssim 10^4\,\mathrm{K}$. Massive stars evolve and explode in a few million years as supernovae (SNe), and the SN remnants propagate to form a low-density hot cavity. The expansion of the over-pressure cavities through the ambient medium compresses and sweeps out material in the shock front to produce a bubble-like structure. If the rate of energy input is large enough, the bubbles will form super-bubbles to become Rayleigh-Taylor unstable, and break up the ISM into cloudlets and filaments to create a wind, i.e., large-scale bulk motions in the ISM. We assume such bulk motion to be responsible for the observed superwinds and mass outflows. Because of the complexities of the process involved when bubble-like structures evolve into super-bubbles (Koo & McKee 1992; Wang 1995), which is still poorly known, we just relate the bubbles to galactic winds directly in the present paper because the radiative cooling does not play an important role here (Heckman et al. 2001; Hoopes et al. 2003) and conservation of specific enthalpy will enable us to establish this direct link (E2000).

In such a scenario, the properties of the superwind from a galaxy are expected to depend not only on the properties of the ISM, but also on other properties of the galaxy concerned. It should be pointed out that, observationally, outflow masses due to galactic winds show complicate components, such as warm neutral, ionized and hot gas with a neutral gas dominated mass budget (Heckman et al. 1990, 2000; Adelberger et al. 2003; Shapley et al. 2003), with the different components possibly having very similar speeds (Heckman et al. 2001). Unfortunately, it is impossible for us to investigate the phenomenon in such details due to the complicated physical processes. For simplicity, we assume that the wind velocity for different components is the same and is described by the isothermal sound speed of the hot component (see below), because we are only concerned with the global properties of gas outflows and galactic winds in the present paper. In what follows, we quantify the main processes involved in our model.

2.1 Supernova Evolution, Interstellar Media and Galactic Winds

Star formation generally takes place in giant molecular clouds that consist of many small and dense clouds. The differential number density distribution of clouds (assumed spherical) as a function of cloud radius is assumed to follow a power-law (MO77; E2000)

$$\frac{dN_c}{da} = n_0 a^{-4}, \quad a_\mathrm{l} \le a \le a_\mathrm{u}, \tag{1}$$

where a_l and a_u are lower and upper limits for the cloud radii, and n_0 is a normalization constant. We take, following MO77,

$$a_\mathrm{l} = 0.5\,\mathrm{pc}, \quad a_\mathrm{u}/a_\mathrm{l} = 20. \tag{2}$$

We caution that the exact value of the lower limit radius ($a_{\rm l}$) is unclear. It is generally believed to be in the range of 0.5 to 1 pc (MO77), consistent with the more recent estimates by Olmi & Testi (2002).

It is easy to show by integration that the local cloud number density, $n_{\rm cl}$, is related to n_0 by

$$n_{\rm cl} = n_0/3a_{\rm l}^3, \ \text{for} \ \ a_{\rm u} \gg a_{\rm l}. \tag{3}$$

Writing $\bar{\rho}_{\rm c}$ for the mean mass density within individual clouds, the mean cold gas density $\bar{\rho}_{\rm cold}$ can be written as

$$\bar{\rho}_{\rm cold} = \int_{a_{\rm l}}^{a_{\rm u}} \frac{dN_c}{da}\frac{4\pi}{3}a^3\bar{\rho}_{\rm c}da = \frac{4\pi}{3}\bar{\rho}_{\rm c}n_0{\rm ln}\frac{a_{\rm u}}{a_{\rm l}}. \tag{4}$$

Then, the volume filling factor of the cold gas is

$$f_{\rm c} = \frac{\bar{\rho}_{\rm cold}}{\bar{\rho}_{\rm c}}. \tag{5}$$

If we assume the rest of the volume to be occupied by hot gas, then the porosity P of the hot phase is related to $f_{\rm c}$ by $f_{\rm c} \equiv e^{-P}$.

According to MO77, an expanding SN remnant can evaporate and sweep up the surrounding ISM. The total evaporation mass, which includes hot, warm ionized and warm neutral components as mention above, is

$$M_{\rm ev} = 540\,{\rm E_{51}}^{6/5} n_{\rm h}^{-4/5}\Sigma^{-3/5}\,{\rm M_\odot}, \tag{6}$$

where $\rm E_{51}$ is the energy output by one SN in units of 10^{51}erg, $n_{\rm h}$ is the hot gas density interior to the SN remnant and Σ is the evaporation parameter

$$\Sigma = \frac{\gamma}{4\pi a_{\rm l} n_{\rm cl}\phi_k} = \frac{\gamma a_{\rm l}^2 {\rm ln}(a_{\rm u}/a_{\rm l})}{\phi_k}\frac{\bar{\rho}_{\rm c}}{\bar{\rho}_{\rm cold}}. \tag{7}$$

Here γ is the ratio of the blast wave velocity to the isothermal sound speed of the hot phase, which is usually taken to be 2.5 (valid for strong shocks), and the parameter ϕ_k denotes the efficiency of conduction relative to the classic thermal conductivity of the clouds, which is roughly in the range of 0.1 to 0.01 due to the suppression of heat conduction by tangled magnetic fields (E2000).

As argued by several authors (Silk 1997, 2001, 2002; E2000; Clarke & Oey 2002), star formation in galaxies may proceed in such a way that the porosity P is always maintained at a value close to unity in star formation regions. This constancy in the porosity P is supported by observations in the Milky Way, and can be understood as follows. If the porosity were too large, the cold gas fraction would be small and the star formation activity would be reduced. The hot gas will then cool quickly, and hence leading to a lower porosity. Conversely, if the porosity were too small, the cold gas fraction would be large. As the cooling and dynamical timescales are likely to be short in the star formation regions, star formation will ensue and hence lead to a higher SFR and higher porosity. In the present study, we assume the porosity to be unity everywhere in a star formation region. Observations may indicate that the volume filling factor of cold and hot phase in galactic winds could be different from our assumption for the star forming regions (McCarthy et al. 1987; Heckman et al. 1990), which could have resulted from the assumption bias and the complicated evolution of the bubbles. We will discuss the impact of changing this assumption in Section 2.2.

Adopting $a_{\rm u}/a_{\rm l} = 20$, we can rewrite the evaporation parameter (Σ) as

$$\Sigma = 752 f_{\rm c}^{-1}\left(\frac{\gamma}{2.5}\right)\left(\frac{\phi_k}{0.01}\right)^{-1}\left(\frac{a_{\rm l}}{\rm pc}\right)^2\,{\rm pc}^2. \tag{8}$$

Note that the value of Σ is not very sensitive to the ratio $a_{\rm u}/a_{\rm l}$ because it enters Eq. (8) logarithmically. For convenience, we define a new parameter

$$f_\Sigma = \frac{\Sigma}{\Sigma_\odot}, \qquad \Sigma_\odot = 95\,{\rm pc}^2, \tag{9}$$

which is the evaporation parameter normalized to the value close to the solar neighborhood (E2000). Numerically, we have

$$f_\Sigma = 21.5 \left(\frac{f_{\rm c}}{e^{-1}}\right)^{-1} \left(\frac{\gamma}{2.5}\right) \left(\frac{\phi_k}{0.01}\right)^{-1} \left(\frac{a_{\rm l}}{\rm pc}\right)^2. \tag{10}$$

Following MO77 and E2000, we can also obtain the temperature of the hot gas in the cavities

$$T_{\rm h} = 6.6 \times 10^5 (S_{-13}\,{\rm E}_{51} f_\Sigma/\gamma)^{0.29}\,{\rm K}, \tag{11}$$

and the mass evaporation rate per unit volume

$$\dot\rho_{\rm ev} = 2.7 \times 10^{-10} S_{-13}^{0.71} \gamma^{0.29}\,{\rm E_{51}}^{0.71} f_\Sigma^{-0.29}\,{\rm M_\odot\,pc^{-3}yr^{-1}}, \tag{12}$$

where S_{-13} is defined as the the SN explosion rate in units of $10^{-13}{\rm pc^{-3}yr^{-1}}$. From equations (11) and (12) and the definition of f_Σ [Eq. (9)], we see that the temperature $T_{\rm h}$ and the mass evaporation rate $\dot\rho_{\rm ev}$ are in fact independent of the parameter γ.

As discussed in the previous section, the SN remnants will expand to form bubbles, which compress and heat the ambient ISM in the shock fronts, producing a "wind" with a velocity comparable to the isothermal sound speed of the hot phase. For a fully ionized primordial gas, the isothermal sound speed is

$$C_{\rm i} = (kT_{\rm h}/\mu m_{\rm p})^{1/2} = 37 T_5^{1/2}\,{\rm km\,s^{-1}}\,, \tag{13}$$

where T_5 is the hot gas temperature in units of $10^5\,{\rm K}$ and $\mu = 0.61$ is the mean molecular weight per particle. Because in the conservation of specific enthalpy, the wind will accelerate and reach a bulk terminal speed to form a superwind (E2000). The terminal wind velocity is related to the isothermal sound speed by

$$v_{\rm wind} = \Gamma_{\rm w} C_{\rm i}. \tag{14}$$

We take $\Gamma_{\rm w} \approx \sqrt{2.5}$, instead of $\sqrt{5}$; our value is appropriate when part of the thermal energy is lost radiatively (see appendix B in E2000 for details). Observationally, because normal ISM motions in galaxies are on the order of $\sim 100\,{\rm km\,s^{-1}}$, it is only when the initial sound speed of the hot gas is larger than $\sim 100\,{\rm km\,s^{-1}}$ that galactic winds can be readily observed (e.g. Heckman et al. 2000). Moreover, if the wind speed is too small, the outflow will fall back to form a galactic fountain in a relative short timescale which could be hard to detect. From Eq. (14), this sound speed corresponds to roughly $160\,{\rm km\,s^{-1}}$ in the terminal velocity.

Note that dark matter halos, which dominate the potential wells of galaxies, have not entered our discussions explicitly. Thus, the local properties of outflows, such as wind velocity and evaporation rate per unit volume, depend only on the properties of the star-forming region. This is consistent with the observations of soft X-rays from hot extended gas in galaxies and the detailed analysis of wind velocities by Heckman et al. (2000), who found that terminal velocities of the superwinds are almost independent of the galaxy potential well. However, the dark halo of a galaxy will play an important role in determining whether the outflow can eventually escape from the galaxy or fall back into the galaxy.

2.2 Model Uncertainties

The model presented above makes several simplified assumptions about the properties of the ISM. In this subsection, we discuss how our results may be affected by the uncertainties in these assumptions.

An important assumption in our model is that the porosity P is close to unity. While this seems to be supported by observations, it is hard to justify from first principles (Silk 1997, 2001), and it is important to examine the dependence of our results on the value of P. Clarke & Oey (2002) claimed the existence of a critical value of the SFR, $\sim 0.15\,\mathrm{M_\odot\,yr^{-1}}$, for star-forming systems, above which galaxies can achieve $P \sim 1$ after a time

$$t_{\rm Q} = t_{\rm e}\left(\frac{\rm SFR_{crit}}{\rm SFR}\right)^{1/2}, \tag{15}$$

where $t_{\rm e} \sim 40\,\mathrm{Myr}$. Since almost all of the star forming galaxies we are interested in have SFR much higher than the critical value, the assumption $P = 1$ should be a reasonable one according to the arguments of Clarke & Oey (2002). Assuming that the hot interstellar gas component in our Galaxy is produced by SN explosions and the associated stellar winds, one may find that the filling factor of the hot gas varies with both radius and altitude in the Milky Way and in external galaxies, and the porosity varies from ~ 0.2 to ~ 1.5 (e.g. Ferriere 1998). In an earlier theoretical study, Heiles (1990) obtained a Galaxy-wide average porosity $P \sim 0.3$. In our model, the wind velocity $v_{\rm wind}$ and mass outflow rate $\dot{\rho}_{\rm ev}$ scale with the porosity as $P^{-1/7}$ and $(1-e^{-P})/[P^{5/7}(1-e^{-1})]$, respectively. For P in the range from 0.2 to 2, the predicted wind velocity changes by less than 25% while the mass outflow rate changes by less than 20% from our canonical results (which assume $P = 1$). Based on these considerations, we conclude that our assumption of $P = 1$ should not have a serious effect on our results.

OB stars, the progenitors of Type II supernovae, generally form in clusters rather than in isolation (e.g. Oey & Clarke 1998; McKee & Williams 1997). The complex interaction between multiple supernova explosions and ISM is difficult to treat. We ignore this complication, as in all previous studies. Also for simplicity we have assumed that the clouds are spherical. Molecular clouds are observed to show very complex structures on large scales; only dense cores, in which stars form, can be considered spherical. Curry (2002) found that the mean intrinsic axis ratio of dense cloud cores is ~ 0.54. This is only a moderate departure from sphericity. On the other hand, the large-scale complexity of the molecular clouds may affect our prediction about the mass evaporation rate. Unfortunately, the details about the propagation of supernova-driven shocks in a realistic ISM are still poorly understood, and so at the moment we have to live with the uncertainty associated with this assumption.

From Equations (11) and (12) we see that the model predictions for the wind properties (velocity and mass outflow rate) depend on the choices of the values of ϕ_k and $a_{\rm l}$. As discussed above, the values of these two parameters are probably in the ranges $0.01 \lesssim \phi_k \lesssim 0.1$ and $0.5\,\mathrm{pc} \lesssim a_{\rm l} \lesssim 1\,\mathrm{pc}$. Using Equations (11) and (12), one can estimate that these ranges correspond to a factor of $\lesssim 2$ in the predicted wind velocity, and a factor of $\lesssim 3$ in the predicted mass outflow rate.

2.3 Star Formation in Galactic Disks

So far we have only considered superwinds and mass outflows launched locally from a particular location in a star formation region. The derived superwinds and mass outflows therefore only depend on the local star formation activities. The observed wind velocity and mass outflow rate from a galaxy should be a proper average and sum of the wind velocity and outflow rate over the whole star formation region. It is these global quantities that can be directly compared

with observation. In this subsection, we consider a simple model where star formation takes place in thin galactic disks. This may be a reasonable assumption, as the cold gas supporting star formation generally has angular momentum and is likely to settle into a rotation-supported thin disk.

For simplicity, we assume the velocity dispersion (σ_g) of the cold clouds in a disk to be constant everywhere. Throughout this paper, we choose σ_g to be $10\,\mathrm{km\,s^{-1}}$, a value consistent with observation (Stark & Brand 1989). The equation of hydrostatic equilibrium gives the following solution of the cold gas density distribution in the vertical direction:

$$\rho(z) = \frac{\mu_{\rm g}}{2H_g}\mathrm{sech}^2\left(\frac{z}{H_g}\right), \tag{16}$$

where $\mu_{\rm g}$ is the cold gas surface density and H_g is the scale height given by

$$H_g = \frac{\sigma_g^2}{\pi G \mu_{\rm g}} = 74\left(\frac{\mu_{\rm g}}{\mathrm{M_\odot\,pc^{-2}}}\right)^{-1}\left(\frac{\sigma_g}{\mathrm{km\,s^{-1}}}\right)^2\ \mathrm{pc}, \tag{17}$$

and G is the gravitational constant (Spitzer 1942).

Kennicutt (1998) studied star formation under a wide range of physical conditions, ranging from quiescent galactic disks to starburst regions. He derived an empirical law for the SFR per unit area as a function of the cold gas surface density,

$$\dot{\mu}_* = 2.5\times10^{-10}\left(\frac{\mu_{\rm g}}{\mathrm{M_\odot\,pc^{-2}}}\right)^{1.4}\mathrm{M_\odot\,yr^{-1}\,pc^{-2}}. \tag{18}$$

It then follows that the SFR density is

$$\dot{\rho}_* \approx \frac{\dot{\mu}_*}{2H_g} = 1.7\times10^{-12}\left(\frac{\mu_{\rm g}}{\mathrm{M_\odot\,pc^{-2}}}\right)^{2.4}\left(\frac{\sigma_g}{\mathrm{km\,s^{-1}}}\right)^{-2}\mathrm{M_\odot\,yr^{-1}\,pc^{-3}}, \tag{19}$$

and the SN explosion rate S_{-13} is

$$S_{-13} = 10^{13}\times\frac{\dot{\rho}_*}{M_{\rm ps}} = 1.35\times10^{-1}\left(\frac{\mu_{\rm g}}{\mathrm{M_\odot\,pc^{-2}}}\right)^{2.4}\left(\frac{\sigma_g}{\mathrm{km\,s^{-1}}}\right)^{-2}\left(\frac{M_{\rm ps}}{125\mathrm{M_\odot}}\right)^{-1}, \tag{20}$$

where $M_{\rm ps}$ is the total mass of star formation required to produce one supernova explosion.

Substituting the above equation into Eqs. (11) and (14), we can infer the wind velocity $v_{\rm wind}$ to be

$$v_{\rm wind} = 150\,\mathrm{km\,s^{-1}}\left(\frac{\mu_{\rm g}}{\mathrm{M_\odot\,pc^{-2}}}\right)^{0.35}\left(\frac{\sigma_g}{\mathrm{km\,s^{-1}}}\right)^{-0.29}\left(\frac{M_{\rm ps}}{125\,\mathrm{M_\odot}}\right)^{-0.15}\mathcal{K}^{0.15}. \tag{21}$$

The corresponding mass outflow rate per unit area can be obtained by multiplying the mass outflow rate per unit volume and the scale height

$$\dot{\mu}_{\rm ev} \approx 2H_g\dot{\rho}_{\rm ev} = 5.1\times10^{-9}\ \mathrm{M_\odot\,yr^{-1}\ pc^{-2}}\left(\frac{\mu_{\rm g}}{\mathrm{M_\odot\,pc^{-2}}}\right)^{0.7}\left(\frac{\sigma_g}{\mathrm{km\,s^{-1}}}\right)^{0.58}\left(\frac{M_{\rm ps}}{125\,\mathrm{M_\odot}}\right)^{-0.71}\mathcal{K}^{-0.29}, \tag{22}$$

where

$$\mathcal{K} = \left(\frac{f_\Sigma}{21.5}\right)\left(\frac{\gamma}{2.5}\right)^{-1} \tag{23}$$

gives the dependence of $v_{\rm wind}$ and $\dot{\mu}_{\rm ev}$ on the properties of the ISM.

As one can see, for given σ_g and $\mathcal{K}$, the wind velocity increases with $\mu_{\rm g}$. Thus, superwinds are more likely to occur in compact systems of cold gas. The wind velocity decreases with σ_g,

because a higher value of σ_g implies a larger disk thickness, and hence a lower density of cold gas. The mass outflow rate per unit area also increases with gas surface density, because of the dependence of the SFR per unit area on the surface density of cold gas. Moreover, according to eq. (25) in E2000 and Eq. (17) above we can estimate that the density of the hot gas in the star forming regions is a few percent of the corresponding cold gas which is consistent with observations although their volume filling factor is comparable.

As discussed in the last subsection, we adopt the lower limit of the wind velocity to be $\sim 160\,\mathrm{km\,s^{-1}}$ which is the lower limit that can lead to an observable superwind (e.g. Heckman 2000). This limit directly translates into a lower limit on the SFR per unit area, which can be obtained from Eq. (21). For the reasonable ranges of ϕ_k and a_1, i.e., $\phi_k = 0.01 - 0.1$ and $a_1 = 0.5 - 1\,\mathrm{pc}$, the limit is about

$$\mathrm{SFR_{th}} \sim 0.01 - 0.05\,\mathrm{M_\odot\,yr^{-1}\,kpc^{-2}}, \tag{24}$$

which, from Eq. (18), corresponds to a cold gas surface density about $10 - 40\,\mathrm{M_\odot\,pc^{-2}}$. This limit is consistent with the observational estimation quoted by Heckman (2001).

The predicted mass outflow rate per unit area as a function of the star formation rate per unit area is shown in Fig. 1. The solid and dashed lines are the results when the lower limit of the cloud radius is chosen to be 0.5 pc and 1 pc, respectively. The thin and thick lines denote the results with the parameter ϕ_k chosen to be 0.01 and 0.1, respectively. For any given ϕ_k and a_1, the mass outflow rate per unit area increases with the SFR per unit area, as pointed out before. Note that the predicted mass outflow rates per unit area are comparable to (or higher than) the SFRs per unit area, which is consistent with observation (Heckman et al. 2000; Pettini et al. 2000, 2001, 2002).

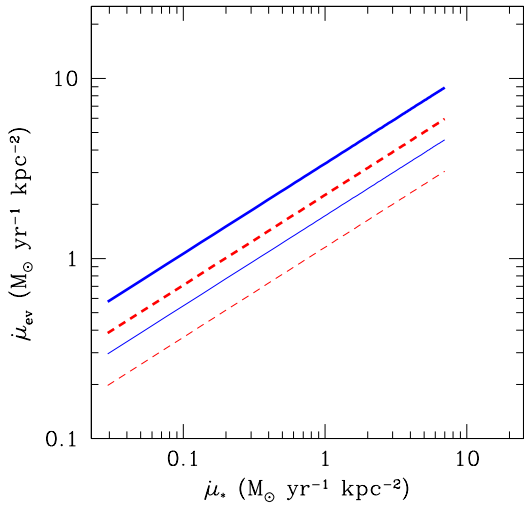

Fig. 1 Predicted mass outflow rate per unit area as a function of the SFR per unit area. The solid and dashed lines are the results where the lower limit of the cloud radius is chosen to be 0.5 pc and 1 pc, respectively. The thin and thick lines denote results with the parameter ϕ_k chosen to be 0.01 and 0.1, respectively. Here the velocity dispersion of the cold gas clouds is assumed to be $10\,\mathrm{km\,s^{-1}}$.

So far we have considered only local properties of winds in galactic disks. To facilitate direct comparison between model predictions and observations, we must consider globally-averaged quantities of the wind. As a simple example, we assume that the cold gas is distributed in an exponential disk

$$\mu_{\rm g} = \mu_0 \exp(-r/r_d), \quad \mu_0 = \frac{M_{\rm g}}{2\pi r_d^2}, \tag{25}$$

where μ_0 is the central surface density of cold gas, $M_{\rm g}$ is the total cold gas mass and r_d is the scale length for the disk. Note that our results are not sensitive to the assumed cold gas surface density distribution because the cold gas surface density enters the wind velocity and mass outflow rate only with moderate power-law indices (0.35 and 0.7) in Eqs. (21) and (22), respectively. Using the star formation law (Eq. 18), one can easily show that the surface density of star formation rate is

$$\dot{\mu}_\star = 2.5 \times 10^{-10} \left(\frac{\mu_0}{\rm M_\odot\,pc^{-2}}\right)^{1.4} e^{-1.4r/r_d}\,{\rm M_\odot\,yr^{-1}\,pc^{-2}}, \tag{26}$$

and the total star formation rate within the disk is

$$\dot{M}_\star = 8.0 \times 10^{-4} \left(\frac{\mu_0}{\rm M_\odot\,pc^{-2}}\right)^{1.4} \left(\frac{R_d}{\rm kpc}\right)^2 {\rm M_\odot\,yr^{-1}}. \tag{27}$$

As discussed above, there is a threshold in the SFR per unit area (Eq. 24), i.e., the lower limit of the cold gas surface density, above which observable galactic winds can be produced. If the central surface density μ_0 for a disk galaxy is lower than this, no observable galactic wind will occur. The threshold implies a critical radius $r_{\rm cr}$ for any given $\mathcal{K}$, beyond which no outflow will occur. The critical radius satisfies

$$\mu_{\rm cr} = \mu_0 \exp(-r_{\rm cr}/r_d). \tag{28}$$

It is easy to calculate the total mass outflow rate within this critical radius

$$\begin{aligned}
\dot{M}_{\rm ev} &= 6.2 \times 10^{-2}\,{\rm M_\odot\,yr^{-1}} \left(\frac{r_d}{\rm kpc}\right)^2 \left(\frac{\mu_0}{\rm M_\odot\,pc^{-2}}\right)^{0.7} \\
&\quad \times \left(\frac{\sigma_g}{\rm km\,s^{-1}}\right)^{0.58} \left(\frac{M_{\rm ps}}{125{\rm M_\odot}}\right)^{-0.71} \mathcal{K}^{-0.29} \mathcal{F}(0.7, \mu_0) \\
&= 9.8\,{\rm M_\odot\,yr^{-1}} \left(\frac{M_{\rm g}}{10^9{\rm M_\odot}}\right) \left(\frac{\mu_0}{\rm M_\odot\,pc^{-2}}\right)^{-0.3} \\
&\quad \times \left(\frac{\sigma_g}{\rm km\,s^{-1}}\right)^{0.58} \left(\frac{M_{\rm ps}}{125{\rm M_\odot}}\right)^{-0.71} \mathcal{K}^{-0.29} \mathcal{F}(0.7, \mu_0)\,,
\end{aligned} \tag{29}$$

where the function $\mathcal{F}(x, \mu_0)$ is defined as

$$\mathcal{F}(x, \mu_0) = 1 - \left[1 - x \ln\left(\frac{\mu_{\rm cr}}{\mu_o}\right)\right] \left(\frac{\mu_{\rm cr}}{\mu_o}\right)^x, \tag{30}$$

where $\mathcal{F}(x, \mu_0)$ describes the fraction of area that contributes to the observable galactic wind. For any given x, $\mathcal{F}$ will first increase with μ_0 for small values of μ_0, and then decrease with increasing μ_0 for large values of μ_0.

The observed superwind velocity is an appropriate average of the wind velocities over the whole disk. Since the mass outflow rate per unit area is proportional to $\mu_{\rm g}^{0.7}$, we define the global wind velocity to be the average of the wind velocities weighted by $\mu_{\rm g}^{0.7}$. This wind velocity is

$$V_{\rm wind} = 68\,{\rm km\,s^{-1}} \left(\frac{\mu_0}{\rm M_\odot\,pc^{-2}}\right)^{0.35} \left(\frac{\sigma_g}{\rm km\,s^{-1}}\right)^{-0.29} \left(\frac{M_{\rm ps}}{125\,{\rm M_\odot}}\right)^{-0.15} \left(\frac{\mathcal{F}(1.05, \mu_0)}{\mathcal{F}(0.7, \mu_0)}\right) \mathcal{K}^{0.15}. \tag{31}$$

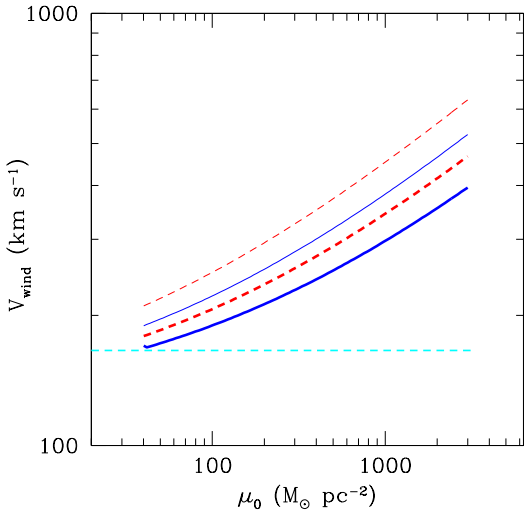

Fig. 2 Predicted mass outflow rate weighted wind velocity as a function of μ_0 where the solid and dashed lines have the same notations as that in Fig. 1 with the dotted horizontal line marking the lower limit of the velocity, $\sim 160\,\mathrm{km\,s^{-1}}$. Here the velocity dispersion of the cold gas clouds is assumed to be $10\,\mathrm{km\,s^{-1}}$.

In reality, the observed wind velocity depends on where the wind originates, and our weighting scheme can only serve as an approximation. We have also made calculations using a weighting proportional to $\mu_{\rm g}$ and to $\mu_{\rm g}^{1.4}$ (i.e. to the surface density of SFR). The results for these three weighting schemes differ only by 20%. Note that for a given $\mathcal{K}$ the wind velocity for an exponential disk depends only on the central surface density of cold gas, while the total mass outflow rate for the disk depends in addition on the scale length (or the total cold gas mass).

Figure 2 shows the predicted global wind velocity for an exponential disk with $\mu_0 \gtrsim \mu_{\rm cr}$ as a function of the cold gas central surface density μ_0 for four different combinations of ϕ_k and $a_{\rm l}$. The notation of the figure is the same as that in Fig. 1 with the dotted horizon line marking the lower limit of the velocity, $\sim 160\,\mathrm{km\,s^{-1}}$, as discussed above. For given ϕ_k and $a_{\rm l}$, the predicted global wind velocity increases with the cold gas surface density μ_0. Galaxies with low cold gas surface density (e.g., low surface brightness galaxies or high-surface brightness galaxies with low cold gas surface density such as our Milky Way) will not produce observable galactic winds because their star formation rate is too low.

As an example, Fig. 3 plots the predicted total mass outflow rate (solid lines) and the corresponding SFR (dashed lines) as a function of μ_0 with (a) and (b) for (ϕ_k, $a_{\rm l}$) equal to (0.01, 1 pc) and (0.1, 0.5 pc), respectively. The lines from top to bottom are for total cold gas mass $2\times10^{11}\,\mathrm{M_\odot}$, $2\times10^{10}\,\mathrm{M_\odot}$ and $2\times10^{9}\,\mathrm{M_\odot}$, respectively. From the figure we see that the cold gas central density μ_0 must be larger than a critical value $\mu_{\rm cr}$ (about 10 and $40\,\mathrm{M_\odot\,pc^{-2}}$ for the values of ϕ_k and $a_{\rm l}$ adopted here respectively) for an observable wind to occur. If $\mu_0 < \mu_{\rm cr}$, no observable galactic wind will be produced no matter how large the total cold gas mass is.

For $\mu_0 \gtrsim \mu_{\rm cr}$, the total mass outflow rate increases with the total mass of cold gas for a given μ_0 because of the increase of the SFR and the star formation region that can produce observable outflows. For a given total cold gas mass, the predicted mass outflow rate first increases rapidly

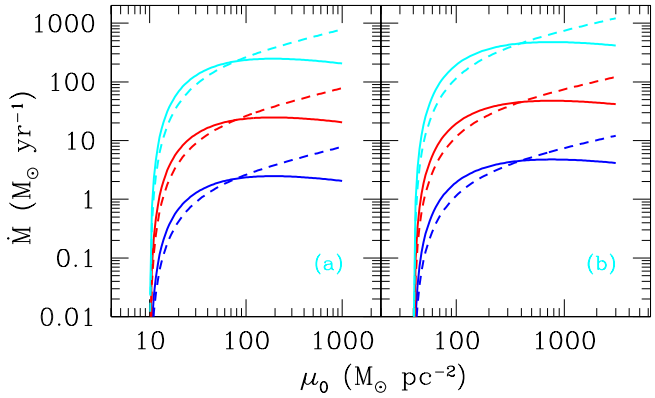

Fig. 3 Predicted mass outflow rate (solid lines) and the corresponding star formation rate (dashed lines) as a function of μ_0 for given the total cold gas mass, where the lines from top to bottom are for total cold gas mass of $2 \times 10^{11}\,M_\odot$, $2 \times 10^{10}\,M_\odot$ and $2 \times 10^{9}\,M_\odot$, respectively. Here the velocity dispersion of the cold gas clouds is assumed to be $10\,km\,s^{-1}$, (a) and (b) present the results for (ϕ_k, a_1) equal to (0.01, 1 pc) and (0.1, 0.5 pc), respectively.

with μ_0, because the gas mass that can produce observable winds [i.e. r_{cr} in Eq. (28)] increases with μ_0. The mass outflow rate as a function of μ_0 reaches a plateau and then decreases when μ_0 is larger than $\sim 10^3\,M_\odot\,pc^{-2}$. This happens because when μ_0 is high enough, the total gas mass that can produce observable galactic winds is saturated while the SFR density increases with increasing μ_0. This increase in SFR density reduces the mass outflow rate, again because the increase of $\dot{\rho}_{ev}$ with SFR density is slower than linear (see Eq. (12)). Note that the predicted mass outflow rates are comparable to the SFR for a very wide range of μ_0, which is consistent with current observations.

3 COMPARISONS WITH OBSERVATIONS

As stated in the Introduction, many observational studies have investigated galactic winds both in local starburst galaxies and in high-redshift star forming galaxies. In this section, we examine whether the predictions of our model can match the current observational data. It should be noted that the comparisons done here only focus on the wind speeds for local starburst galaxies, and on both the amount of mass of the outflows and the wind speeds for high redshift star forming galaxies. Although there are now many other observational results available, one cannot compare the model results with individual detailed observations such as the temperatures of the outflows because of the simplicity of the model as mentioned above.

Although the shapes of star forming regions are very complicated, they are all disk-like observationally ranging from quiescent disks to starburst galaxies as discussed by Kennicutt (1998). Moreover, the prescriptions of the galactic winds and mass outflows given in Eqs. (21) and (22), Eqs. (29) and (31) are all proportional to the gas surface density with power indexes smaller than unity. This means that our results will not be very sensitive to the assumption that star forming regions are disk-like.

For definiteness, we will adopt $\phi_k = 0.01$ and $a_1 = 1\,pc$ throughout this section. As we discussed in Sect. 2.1, other plausible choices of these parameters may result in a lower wind

velocity by a factor of $\lesssim 2$ and a higher mass outflow rate by a factor of $\lesssim 3$. The choice is quite arbitrary, since the exact values of ϕ_k and a_1 appropriate for star forming galaxies are not known *a priori*. Our chosen values do give reasonable agreement with the observational results to be discussed below.

3.1 Local Starburst Galaxies

Based on the Na D absorption lines, Heckman et al. (2000) estimated galactic wind velocities for local starburst galaxies. They found that the wind velocities are in the range of 400 to $800\,\mathrm{km\,s^{-1}}$. They also estimated mass outflow rates, which they claimed to be comparable to the SFRs. The observational results for the mass outflow rates are only qualitative and we have shown that they are consistent with our model predictions. In what follows, we will primarily focus on the wind velocities which are more accurately determined.

We can estimate the global galactic wind velocities for these galaxies using Eq. (21), provided that their SFRs and sizes are known (so that μ_0 can be estimated using Eq. (27)). To be specific we define the size of a star forming galaxy with exponential profile to be the radius within which half of the star formation activity is contained. We estimate the SFRs for these starburst galaxies using their FIR luminosities (Kennicutt 1998):

$$\frac{\mathrm{SFR}}{\mathrm{M_\odot\,yr^{-1}}} = \frac{L_{\mathrm{FIR}}}{5.8\times 10^9 L_\odot}. \tag{32}$$

The sizes of the star forming regions for the galaxies in consideration are not available. As a rough estimate, we take the sizes to be the same as the observational slit widths, which, according to Heckman et al. (2000), is a reasonable match to the typical sizes of powerful starbursts. The observational data are from table 4 in Heckman et al. (2000). The predicted wind velocities are plotted versus the observed velocities in Fig. 4 (the crosses). The line in the figure marks perfect agreement. It should be noted that the observations have large uncertainties of $\sim 100\,\mathrm{km\,s^{-1}}$ (Heckman et al. 2000). As can be seen, our model predictions roughly match the observations within the model and observational uncertainties.

Another way to empirically estimate the superwind velocities for galaxies is based on X-ray observations. Galactic winds will spread out the hot gas within the galactic halos and contribute to the soft component of extended X-ray emission. As the hot gas temperature can be inferred from X-ray observations (e.g., from ROSAT or ASCA), we can estimate the wind velocities from the temperature of the soft X-ray components using Eq. (11). The galaxies we selected are similar to those in Heckman et al. (2000). They are NGC 4449 (Della Ceca, Griffiths & Heckman 1997), NGC 2146 (Della Ceca et al. 1999), NGC 253, NGC 3079, M82, NGC 4631 (Dahlem, Weaver & Heckman 1998), NGC 1569 (Della Ceca et al. 1996), Arp 299 (Heckman et al. 1999), NGC 6240 (Iwasawa & Comastri 1998), NGC 1808 (Awaki et al. 1996). Note that we assume the relation between wind velocity and soft X-ray temperature to be $V_{\mathrm{wind}} = \sqrt{2.5kT_{\mathrm{X}}}$ rather than $\sqrt{5kT_{\mathrm{X}}}$, the relation adopted by Heckman et al. (2000). The reason for our choice is discussed below Eq. (14).

We can estimate the SFRs of these galaxies based on their FIR luminosities according to Equation (32). The sizes of their star formation regions are adopted from the relevant Hα observations, which can be found in the references listed above. The predicted wind velocities can then be obtained using Eq. (31). The open squares in Fig. 4 indicate the predicted wind velocities and the estimated values from the X-ray observations. We find that the predictions match the estimated values reasonably well.

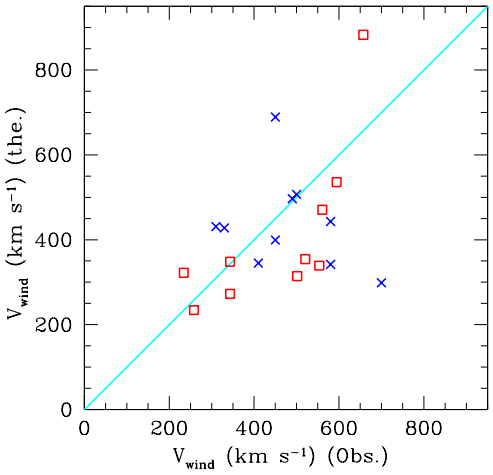

Fig. 4 Predicted vs observed wind velocities for local starburst galaxies. Crosses mark observations of Na D absorption lines with uncertainties of $\sim 100\,\mathrm{km\,s^{-1}}$ and open squares, the estimated results based on the hot gas temperatures from ROSAT and ASCA. The line marks perfect agreement between the observations and model predictions.

3.2 Lyman Break Galaxies

The UV dropout method has been very successful in identifying active star forming galaxies (Lyman break galaxies, hereafter LBGs) at a redshift of $z \approx 3$ (Steidel, Pettini & Hamilton 1995). Their physical nature has been investigated in many observational and theoretical studies (see Mo & Fukugita 1996; Mo, Mao & White 1999; Kauffmann et al. 1999; Katz, Hernquist & Weinberg 1999; Shu 2000; Shu, Mao & Mo 2001). Based on observations of Lyman alpha and nebular emission lines, the LBGs are also inferred to display galactic winds (Pettini et al. 2001; 2002; Adelberger et al. 2002) over a wide range, from 250 to nearly $1000\,\mathrm{km\,s^{-1}}$ with a median value about 500–600 $\mathrm{km\,s^{-1}}$. As for local starburst galaxies, the mass outflow rates for LBGs are difficult to establish observationally. Pettini et al. (2000, 2002) measured a mass outflow rate of $\sim 60\,\mathrm{M_\odot\,yr^{-1}}$ for one particular LBG, the gravitationally lensed (and magnified) system MS 1512-cB58; the outflow rate is comparable to its SFR obtained from its UV luminosity.

Assuming that the cold gas in star forming galaxies has an exponential profile, we can use the model described in Sect. 2.3 to predict the wind properties for the LBG population. The observational inputs are SFRs and sizes of Lyman break galaxies, which can be obtained by Monte Carlo simulations according to their dust-corrected UV luminosity function and the observed size distribution (see Shu, Mao & Mo 2001). Whenever the SFR and half-SFR radius (size) of a Lyman break galaxy is obtained, we can obtain its gas central surface density and scale length by Equations (26) and (27). According to Equations (29) and (31), we can obtain its mass outflow rate and galactic wind velocity. The predicted distributions of the galactic wind velocities and the corresponding mass outflow rates are shown in Figs. 5 and 6, respectively. It can be seen that the median value of the predicted wind velocities for LBGs is ~ 600 $\mathrm{km\,s^{-1}}$, and the median value of the predicted mass outflow rates is about $60\,\mathrm{M_\odot\,yr^{-1}}$. Both are consistent with the observations.

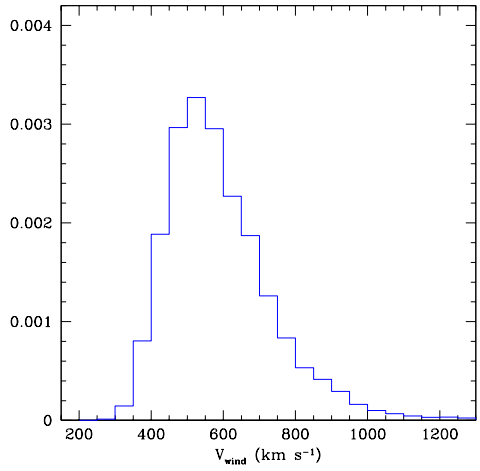

Fig. 5 Predicted distribution of galactic winds for LBGs, assuming the star forming galaxies to be exponential disks.

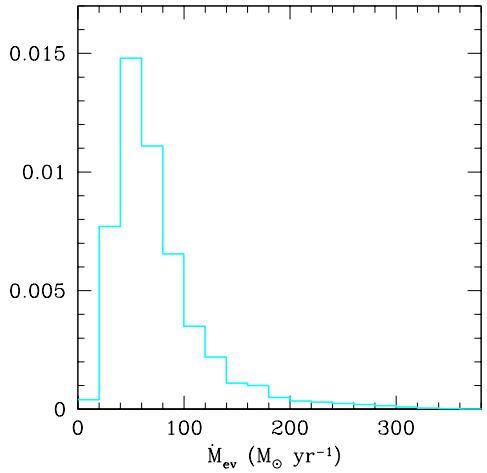

Fig. 6 Predicted distribution of mass outflow rates for LBGs, assuming the star forming galaxies to be exponential disks.

4 ESCAPING GALACTIC WIND AS A FUNCTION OF $V_{\rm C}$ AND REDSHIFT

As we discussed in Sect. 2, galaxies with more compact cold gas distributions (and hence more compact star formation activity) will produce stronger galactic winds. Galactic winds will thus occur preferentially in local starburst galaxies and high redshift galaxies. If the speed of a galactic wind is smaller than the escape velocity of the host galaxy, the mass outflow will fall back into the galaxy and form a galactic fountain. Otherwise, the outflow will escape from the host. This we call an "escaping" outflow. The mechanical energy of the outflow can heat the intergalactic medium (IGM) while heavy elements contained in the wind can chemically enrich this gas. It is therefore important and interesting to estimate the fraction of galaxies (by number) that have escaping outflows at different redshifts. We address this question in the currently preferred ΛCDM cosmogony with a matter density $\Omega_m = 0.3$, a cosmological constant $\Omega_\lambda = 0.7$, a Hubble constant $h = 70\,{\rm km\,s^{-1}\,Mpc^{-1}}$; the power-spectrum is described by a shape parameter $\Gamma = 0.2$ and the usual normalization constant $\sigma_8 = 0.9$.

We assume that the distribution of cold gas within a galaxy is exponential; our results will not change significantly if we adopt other profiles (see Sect. 2.3). We use Mo, Mao & White (1998) to model the formation of disks in dark matter haloes. In this model, the disk properties are determined by the halo circular velocity, $V_{\rm c}$, a dimensionless spin parameter, λ, and the fraction of total mass ($m_{\rm g}$) that settles into the exponential disk. The spin parameter follows a log-normal distribution with a median $\bar{\lambda} = 0.05$ and a dispersion $\sigma_{\ln\lambda} = 0.5$ (e.g., Warren et al. 1992; Lemson & Kauffmann 1999). Once these three parameters ($V_{\rm c}, \lambda$, and $m_{\rm g}$) are specified, the disk properties and hence the star formation and outflow properties can be evaluated using the formalism developed here. In Fig. 7, we show the number fraction of galaxies with escaping winds occurring in the disks as a function of the circular velocity at six different redshifts. For each redshift, four solid lines are plotted, corresponding to four different $m_{\rm g}$ values. Note that, for these results, we have averaged over the spin parameter distributions. In the same figure, we

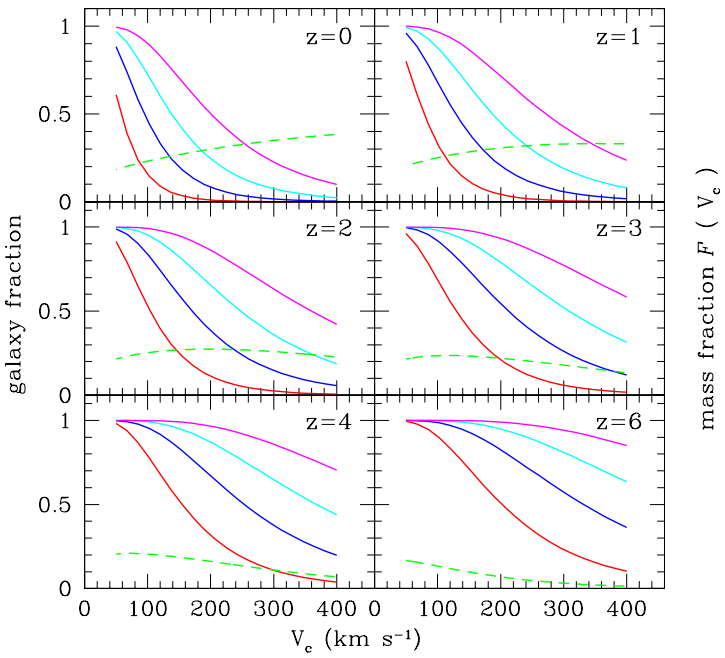

Fig. 7 Predicted fraction of galaxies where superwinds escape from their dark matter haloes is shown as a function of circular velocity at six different redshifts. In each panel, the four solid lines correspond to a gas faction of $m_{\rm g}$ =0.1, 0.05, 0.025 and 0.01 (from top to bottom), respectively. The predicted mass fraction $F(V_{\rm c})$ in halos per logarithmic decade (cf. Eq. (33)) as a function of $V_{\rm c}$ is shown as a dashed line at each redshift in the current ΛCDM cosmogony.

also show the mass fraction $F(V_{\rm c})$ in halos as a function of the circular velocity $V_{\rm c}$ in logarithmic bins at different redshifts, i.e.,

$$F(V_{\rm c}) = \frac{dF(>V_{\rm c}, z)}{d\log {\rm V_c}}, \tag{33}$$

where $F(>V_{\rm c}, z)$ is the mass fraction in haloes with circular velocity larger than $V_{\rm c}$ as predicted by the updated Press-Schechter formalism (c.f. Mo & White 2002). From the dashed line, one can easily estimate the mass fraction of total halos and the typical halo circular velocity which will produce escaping mass outflows.

As expected, for any given $m_{\rm g}$, a larger fraction of small halos produces escaping outflows at any redshift because of their shallower potential wells. Hence, during their evolution, a significant fraction of their baryons will be lost due to the galactic winds. It also implies that most small halos in the local universe are dark matter dominated which is consistent with observation (e.g. Persic, Salucci & Stel 1996). Given $V_{\rm c}$, galaxies with larger $m_{\rm g}$ have a larger probability to produce an escaping outflow at any redshift because of their more active star formation. As the redshift increases, more and more galaxies produce escaping outflows because of the increase in their SFR densities. For example at $z = 3$, more than 80% galaxies with $V_{\rm c} \lesssim 200\,{\rm km\,s^{-1}}$ will produce mass outflows that escape for $m_{\rm g} \gtrsim 0.05$. Hence escaping outflows will occur commonly in LBGs because the median value of their circular velocity is about $150\,{\rm km\,s^{-1}}$ and their $m_{\rm g}$ may be $\gtrsim 0.06$ (Shu, Mao & Mo 2001). Hence, a significant number of galaxies will contribute to the heating of the IGM or ICM. Subsequent galaxy formation

therefore will occur in preheated intergalactic media, as argued by Mo & Mao (2002). Galactic winds therefore should be taken into account for high-redshift galaxies.

As a comparison, it is interesting to study how the star formation rate is partitioned in haloes with different circular velocities. Specifically, we study the differential probability distribution of star formation rate in logarithmic scales of $V_{\rm c}$, i.e.,

$$f(V_{\rm c})d\log {\rm V_c} = \frac{{\rm SFR(V_c)}}{\int {\rm SFR(V_c)d\log V_c}} d\log {\rm V_c}, \tag{34}$$

where SFR is the star formation rate in galaxies for a given circular velocity $V_{\rm c}$ averaged over all spin parameter distributions. Note that this distribution function is normalized to unity for $V_{\rm c}$ between 30 $\rm km\,s^{-1}$ and 400 $\rm km\,s^{-1}$.

We define the cumulative probability distribution function of galaxies with escaping outflows, $f_{\rm ro}(< V_{\rm c})$, as a function of $V_{\rm c}$,

$$f_{\rm ro}(< V_{\rm c}) = \frac{\int_{30}^{V_{\rm c}} {\rm SFR_{esc}(V_c)dV_c}}{\int_{30}^{400} {\rm SFR(V_c)dV_c}}, \tag{35}$$

where $\rm SFR_{esc}$ is the star formation rate in galaxies with escaping outflows for a given circular velocity $V_{\rm c}$.

To obtain these two probability distributions, we have assumed that all galaxies are disk galaxies. Furthermore, the gas fraction $m_{\rm g}$ in the disks is taken to be the fraction of gas that eventually cool in their host haloes; we take the cooling function from Sutherland & Dopita (1993) assuming a metallicity of 0.01 the solar value. The influence of the feedback on $m_{\rm g}$ is also taken into account by adopting

$$m_{\rm g} = \frac{m_{\rm g0}}{1 + (150\,{\rm km\,s^{-1}}/V_{\rm c})^2}\,, \tag{36}$$

as suggested by Dekel & Silk (1986) and White & Frenk (1991). Here $m_{\rm g0}$ is the maximum baryon fraction that can cool in the haloes to form disks.

We show the two probability distributions in Figs. 8 and 9 for six different redshifts, respectively. We can see from Fig. 8 that the SFR fraction of galaxies peaks at $V_{\rm c} \sim 100$–$200\,\rm km\,s^{-1}$ at redshift $z > 1$. However, at lower redshift, most of the SFR is contributed by more massive galaxies because the feedback at low redshift is not as efficient and most baryons within massive halos can cool to form stars. From Fig. 9, we see that the contribution of SFR for galaxies with escaping outflows is dominated by galaxies with $V_{\rm c} \sim 200\,\rm km\,s^{-1}$ at redshift $z \lesssim 3$, while at higher z significant contribution comes from systems with $V_{\rm c} \sim 150\ \rm km\,s^{-1}$. This is because, although at lower redshift the SFR is shifted toward systems with higher $V_{\rm c}$, escaping superwinds are more difficult to produce in these systems. At $z > 3$, more than 40% of all stars are formed in systems where escaping winds are expected. Note that a change in the value of $m_{\rm g0}$ does not affect the result significantly. At high redshift, the number density of high $V_{\rm c}$ systems goes down rapidly and so not many stars can form in these systems.

5 SUMMARY

In this paper, we develop a simple analytic model to understand superwinds and mass outflows that are observed in local starburst galaxies and high-redshift star-forming galaxies. Our scenario is based on the model of McKee & Ostriker (1977) for the evolution of SN remnants in the ISM, which is similar to Efstathiou (2000). Model uncertainties are discussed in detail. We show that the properties of superwinds, such as wind velocity and mass outflow rate, depend not only on the properties of the ISM, but also on the global properties of star forming galaxies. Our main conclusions are:

– Observable winds are produced only in systems where the density of SFR is higher than some threshold. This is consistent with the observational results given by Heckman (2001) and Heckman et al. (2000), and implies that low surface-brightness galaxies and high surface-brightness galaxies with low cold gas surface density cannot produce large-scale superwinds.
– The velocity of superwinds driven by SN explosions depends only on the SFR density. Galaxies in which current star formation is confined in a more compact region can produce winds with higher velocity. This implies that superwinds are expected in local starbursts and in high-redshift star-forming galaxies. The mass outflow rate depends, in addition, on the size of star formation region; a larger star formation region allows more mass to be loaded in the wind.
– The predicted mass outflow rates are comparable to or higher than the corresponding SFRs, consistent with current observations both for local starburst galaxies (Heckman et al. 2000) and for high redshift star-forming galaxies (Pettini et al. 2000, 2001, 2002).
– The predicted wind velocity and outflow rate have no explicit dependence on the properties of dark halos which dominate the potential wells. Thus, galactic winds and mass outflows can occur in a variety of halos, provided that the cold gas density is high enough. This is in agreement with the observation that there is no strong correlation between wind properties and the total mass of a galaxy (Heckman et al. 2000). The potential well of a galaxy will, however, determine whether the outflows escape from the galaxy or will fall back.
– The fraction of galaxies with superwinds that will eventually escape from their dark matter haloes is a function of the circular velocity and the redshift. Our model predicts that the fraction is high in low circular velocity systems such as dwarf galaxies although their contribution to the total SFR is small. More interestingly, we find that the fraction is high for galaxies at high redshifts, such as the LBGs at redshift $z = 3$. The winds will undoubtedly heat and chemically contaminate the IGM, and hence have important implications for subsequent galaxy formations in the preheated IGM.

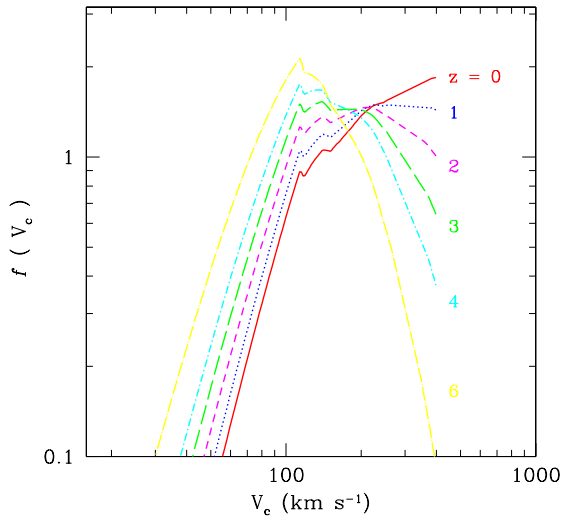

Fig. 8 Predicted fraction of galaxies weighted by the SFR as a function of circular velocity at six different redshifts. Gas cooling and feedback effect have been taken into account and the currently favoured ΛCDM cosmogony is adopted (see text for details).

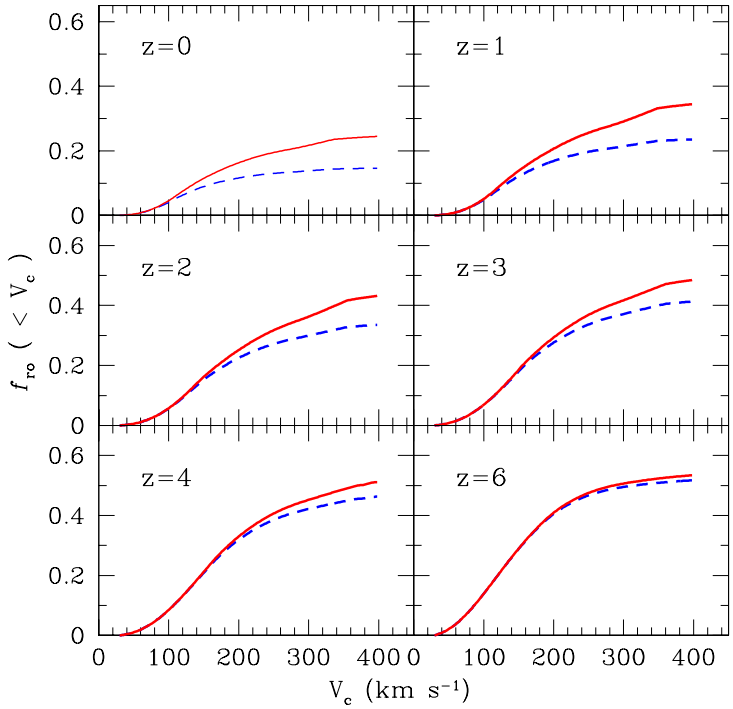

Fig. 9 Predicted cumulative fraction of galaxies with escaping outflows as a function of halo circular velocity at six different redshifts (cf. Eq. (35)). For each redshift, the solid and dashed lines denote results for m_{g0} =0.1 and 0.05, respectively. Gas cooling and feedback effect have been taken into account and the currently favoured ΛCDM cosmogony is adopted (see text for details).

We apply our model to make predictions on the properties of the winds expected from local starburst galaxies and high-redshift Lyman-break galaxies. These predictions can match many of the observed properties. We therefore believe that our model catches the main points required to model the superwind phenomenon. Our model is also simple, and so can be easily incorporated into numerical simulations and semi-analytical models of galaxy formation.

Acknowledgements We thank Simon White for carefully reading the manuscript and useful suggestions. CS acknowledges the financial support of MPG for a visit to MPA. This project is partly supported by the National Natural Foundation of China (10333020), the Chinese National Key Project NKBRSF (G1999075406), Shanghai Natural Science Foundation (03XD14014) and Shanghai Key-Lab (04dz05905).

References

Adelberger K. L., Steidel C. C., Shapley A. E., Pettini M., 2002, preprint (astro-ph/0210315)
Awaki M., Ueno S., Koyama K., Tsuru T., Iwasawa K. 1996, PASJ, 48, 409
Bertone S., Stoehr F., White S. D. M., 2004, preprint (astro-ph/0402044)
Chevalier R. A., Clegg A. W., 1985, Nature, 317, 44
Clarke C. J., Oey M. S., 2002, preprint (astro-ph/0208442)
Curry C. L., 2002, ApJ, 576, 849
Dahlem M., Weaver K., Heckman T., 1998, ApJS, 118, 401
Dawson S., Spinrad H., Stern D. et al., 2002, ApJ, 570, 9
Dekel A., Silk J., 1986, ApJ, 303, 39
Della Ceca R., Griffiths R., Heckman T., MacKenty J., 1996, ApJ, 469, 662
Della Ceca R., Griffiths R., Heckman T., 1997, ApJ, 485, 581
Della Ceca R., Griffiths R., Heckman T., Lehnert M., Weaver K., 1999, ApJ, 514, 772
Efstathiou G., 2000, MNRAS, 317, 697 (E2000)
Ferriere K., 1998, ApJ, 503, 700
Ferrara A., Pettini M., Shchekinov Y., 2000, MNRAS, 319, 539
Forbes D. A., Polehampton E., Stevens I. R., Brodie J. P., Ward M. J., 2000, MNRAS, 312, 689
Furlanetto S. R., Loeb A., 2002, preprint(astro-ph/0211496)
Heckman T. M., Sembach K. R., Meurer G. R., Strickland D. K., Martin C. L., Calzetti D., Leitherer C., 2001, ApJ, 554, 1021
Heckman T. M., 2001, ASP Conf., 254, 292
Heckman T. M., Lehnert M. D., Strickland D. K., Armus L., 2000, ApJS, 129, 493
Heckman T., Armus L., Weaver K., Wang J., 1999, ApJ, 517, 130
Heckman T., Armus L., Miley G. K., 1990, ApJS, 74, 833
Heiles C., 1990, ApJ, 354, 483
Iwasawa K., Comastri A., 1998, MNRAS, 297, 1219
Martin C. L., Kobulnicky H. A., Heckman T. M., 2002, ApJ, 574, 663
Katz N., Hernquist L., Weinberg D. H., 1999, ApJ, 523, 463
Kauffmann G., Colberg J. M., Diaferio A., White S. D. M., 1999, MNRAS, 303, 188
Kennicutt Jr. R. C., 1998, ApJ, 498, 541
Koo B. -C., McKee C. F., 1992, ApJ, 338, 103
Lemson G., Kauffmann G., 1999, MNRAS, 302, L111
Mac Low M., Ferrara A., 1999, ApJ, 513, 142
McCarthy P. J., van Breugel W., Heckman T. M., 1987, AJ, 93, 246
McKee C. F., Williams J. P., 1997, ApJ, 476, 144
McKee C. F., Ostriker J. P., 1977, ApJ, 218, 148 (MO77)
Mo H. J., Fukugita M., 1996, ApJ, 467, L9
Mo H. J., Mao S., White S. D. M., 1998, MNRAS, 295, 319
Mo H. J., Mao S., White S. D. M., 1999, MNRAS, 304, 175
Mo H. J., Mao S., 2002, MNRAS, 333, 768
Mo H. J., White S. D. M., 2002, MNRAS, 336, 112
Oey M. S., Clarke C. J., 1998, AJ, 115, 1543
Olmi L., Testi L., 2002, A&A, 392, 1053
Persic M., Salucci P., Stel F., 1996, MNRAS, 281, 27
Pettini M., Samantha A. R., Steidel C. C., Adelberger K. L., Hunt M. P., Shapley A. E., 2002, ApJ, 569, 742
Pettini M., Shapley A. E., Steidel C. C., Cuby J., Dickinson M., Moorwood A. F. M., Adelberger K. L., Giavalisco M., 2001, ApJ, 554, 981
Pettini M., Steidel C. C., Adelberger K. L., Dickinson M., Giavalisco M., 2000, ApJ, 528, 96

Scannapieco E., Ferrara A., Madau P., 2002, ApJ, 574, 590
Scannapieco E., Ferrara A., Broadhurst T., 2000, ApJ, 536, L11
Shen S., Mo H. J., Shu C., 2001, MNRAS, 331, 259
Shu C. 2000, A&A, 354, 815
Shu C., Mao S., Mo H. J., 2001, MNRAS, 327, 895
Silk J., 1997, ApJ, 481, 703
Silk J., 2001, MNRAS, 324, 313
Silk J., 2002, preprint(astro-ph/0212068)
Spitzer L. Jr., 1942, ApJ, 95, 329
Stark A. A., Brand J., 1989, ApJ, 339, 763
Steidel C. C., Pettini M., Hamilton D., 1995, AJ, 110, 2519
Strickland D. K., Heckman T. M., Weaver K. A., Hoopes C. G., Dahlem M., 2002, ApJ, 568, 689
Strickland D. K., Stevens I. R., 2000, MNRAS, 314, 511
Suchkov A. A., Balsara D. S., Heckman T. M., Leitherner C., 1994, ApJ, 430, 511
Theuns T., Viel M., Kay S., Schaye J., Carswell R. F., Tzanavaris P., 2002, ApJ, 578, L5
Tomisaka K., Bregman J. N., 1993, PASJ, 45, 513
Wang B., 1995, ApJ, 444, 590
Warren M. S., Quinn P. J., Salmon J. K., Zurek W. H., 1992, ApJ, 509, 19
White S. D. M., Frenk C. S., 1991, ApJ, 379, 52
White M., Hernquist L., Springel V., 2002, ApJ, 579, 16